

SCIENTIFIC REPORTS

OPEN

Differences on photosynthetic limitations between leaf margins and leaf centers under potassium deficiency for *Brassica napus* L.

Received: 16 September 2015

Accepted: 29 January 2016

Published: 23 February 2016

Zhifeng Lu^{1,2}, Tao Ren^{1,2}, Yonghui Pan^{1,2}, Xiaokun Li^{1,2}, Rihuan Cong^{1,2} & Jianwei Lu^{1,2}

Analyzing the proportions of stomatal (S_L), mesophyll conductance (MC_L) and biochemical limitations (B_L) imposed by potassium (K) deficit, and evaluating their relationships to leaf K status will be helpful to understand the mechanism underlying the inhibition of K deficiency on photosynthesis (A). A quantitative limitation analysis of K deficiency on photosynthesis was performed on leaf margins and centers under K deficiency and sufficient K supply treatments of *Brassica napus* L. Potassium deficiency decreased A , stomatal (g_s) and mesophyll conductance (g_m) of margins, S_L , MC_L and B_L accounted for 23.9%, 33.0% and 43.1% of the total limitations. While for leaf centers, relatively low limitations occurred. Nonlinear curve fitting analysis indicated that each limiting factor generated at same leaf K status (1.07%). Although MC_L was the main component of limitations when A began to fall, B_L replaced it at a leaf K concentration below 0.78%. Up-regulated MC_L was related to lower surface area of chloroplasts exposed to intercellular airspaces (S_c/S) and larger cytosol diffusion resistance but not the cell wall thickness. Our results highlighted that photosynthetic limitations appear simultaneously under K deficiency and vary with increasing K deficiency intensity.

Potassium (K), one of the macronutrients essential for plant growth and development, is involved in many physiological processes, such as photosynthesis, enzyme activation, water relations, assimilate transport, and protein synthesis^{1,2}. K deficiency profoundly decreased crop yield^{3,4}, thus strategies of survival and improvement would be important for plant growing under adverse conditions. It is a truism that most of the dry matter is formed by leaf photosynthesis (A) which is intimately connected with K status. Multifarious studies have come to a nearly consistent conclusion that leaf A decreases in K-starved plants^{3,5,6}, therefore an even deep comprehending of mechanism underlying the inhibition of K deficiency on A is necessary².

During photosynthesis, CO_2 moves from external atmosphere to the internal leaf air spaces through the stomata, and from there to carboxylation sites inside the chloroplasts⁷. It is established that stomatal closure is the foremost limitation to CO_2 assimilation due to the vital role of K in stomatal aperture^{8,9}. As a major osmotic, K^+ accumulation in vacuole is essential for stomatal opening, which had been verified to be initially dropped under K deficiency¹⁰. And because of this, Bednarsz *et al.*⁵ stated that the most limiting resistance to A of *Gossypium hirsutum* L. came from stomata⁵. In contrast, K starvation caused a decreased A and stomatal conductance (g_s), but an increased intercellular CO_2 concentration (C_i) of *Carya cathayensis* leaves, suggesting that, in addition to g_s , mesophyll conductance (g_m) and biochemical limitations might be involved in the depression of photosynthesis in K deficient conditions⁶. Numerous studies have shown that g_m is relatively low, leading to great draw-down of chloroplastic CO_2 concentration from C_p , and changed along the variation of water status, nitrogen nutrient, irradiance, temperature and CO_2 concentration^{11–14}. Moreover, leaf structures, specific aquaporins, plasma membrane etc. are involved in the determinations of g_m ¹⁵. K starvation might have reduced aquaporin activity¹⁶ and increased leaf dry mass per unit area (M_A)^{1,17}, therefore, causing a stronger mesophyll diffusion resistance to CO_2 delivery¹⁸. Besides, K nutrition also known to increase the leaf intercellular air space to enhance g_m ¹.

Additionally, biochemical processes may restrain photosynthesis, particularly under severe and/or long-time K starvation^{1,5,6}. It was reported that Rubisco (ribulose-1,5-bisphosphate carboxylase/oxygenase, EC 4.1.1.39)

¹College of Resources and Environment, Huazhong Agricultural University, Wuhan 430070, China. ²Key Laboratory of Arable Land Conservation (Middle and Lower Reaches of Yangtze River) Ministry of Agriculture, Wuhan 430070, China. Correspondence and requests for materials should be addressed to J.L. (email: lunm@mail.hzau.edu.cn)

Treatment	Position	Total dry matter (g)	Individual leaf dry matter (g)	Leaf area (cm ²)	K concentration (% of dry weight)	A (μmol CO ₂ m ⁻² s ⁻¹)
-K	margin	21.1 ± 2.6b ¹	2.31 ± 0.03b	320 ± 4b	0.65 ± 0.02b ²	9.5 ± 0.2b
	center				0.98 ± 0.05a	16.5 ± 0.6a
+K	margin	30.1 ± 1.1a	2.97 ± 0.16a	391 ± 8a	1.32 ± 0.06b ^{3*}	17.0 ± 0.3a*
	center				1.66 ± 0.06a*	17.3 ± 0.7a

Table 1. Effects of K deficiency on plant dry matter, leaf dry matter, leaf area, leaf K concentration, and net CO₂ assimilation rate (A) for the two positions in the fifth fully expanded leaves. Values are mean ± SE of six replications for total dry matter, individual leaf dry matter and leaf area, and of four replications for K concentration and A. ¹Different letters in the same column of total dry matter, individual leaf dry matter and leaf area indicate significant differences between treatments ($P \leq 0.05$). ²Different letters in the same column of K concentration and A indicate significant differences between positions ($P \leq 0.05$). ^{3*}shows significant differences between the two K treatment in same position ($P \leq 0.05$).

activity was decreased under K deficiency, becoming a major limiting factor for photosynthesis in *Oryza sativa* leaves³. Chlorophyll synthesis was observed to be significantly impaired under K deficiency in *Eucalyptus grandis* leaves¹. Moreover, K starvation up-regulated the fraction of electron transport to O₂, resulting in an increased reactive oxygen species (ROS)¹⁹. Carbohydrate accumulation which may feedback regulation of leaf photosynthesis is more easily observed in K starved leaves^{20,21}. Indeed, the relative contributions of these three limiting processes to photosynthesis under K deficiency and the underlying mechanisms have not been fully explored, due to the complicated physiological processes and variation of dominant limiting factors under differ K deficiencies^{2,5}. No matter what the primary cause of decrease A, the discrepancy between researches was believed to be derived from differ physiological K deficiency severities. For this reason, a comprehensive consideration of whole limiting factors and their relationships with leaf K status seems to be important.

In 2005, Grassi and Magnani proposed a method to accurately quantify photosynthetic limitations by separating the relative controls on A resulting from S_p, mesophyll conductance (MC_L) and biochemical limitations (B_L)²². This method has been successfully applied for evaluating the relative control of leaf A under water stress and during their recovery processes, among inter- and intra-species^{13,23–25}. It showed not only great potential for elucidating the magnitude changes of limitations and their dominance in photosynthetic restraints with increasing severity of K deficiency, but also revealing the corresponding critical K concentrations for their transformation.

Winter oilseed rape (*Brassica napus* L.), a model-plant of winter cover crops who needs substantial amount of potassium to growth was used for a deeply aggregate analysis of K deficiency on photosynthetic limitations²⁶. However, malfunction of physiological processes like photosynthesis is hard to be affected when K concentration above the threshold value (1.5% in dry matter, or less)¹⁰. On consideration of the fact that potassium deficiency symptoms, characterized by a chlorosis and even scorch around the periphery can be obviously observed when leaf K concentration below 1.0% in most species²⁷. And the withdrawal K initially occurred at the edge of leaf tip, as tip cells are initially proliferated and oldest²⁸, resulting in different K levels as well as visible distinctions between centers and margins. These natural K gradients are therefore precious for photosynthetic limitation analysis, from which we may seek out the main limiting factors under variable leaf K status and the corresponding threshold values. This phenomenon occurred more frequently under a complex biological and abiological environment system during a long-time and low-temperature wintertide, which may conducive to generate a physiology K deficiency in a K-deficient soil, i.e., it may bring K function into full play^{29,30}. Accordingly, the objectives of the present study were to: (1) estimate the differences of contributions for three limiting factors to photosynthesis between leaf margins and leaf centers, (2) uncover the relationships between photosynthetic limitations and diminishing leaf K status, and therefore the critical K concentration for the predominate restraint transformation, (3) reveal the mechanism underlying the K-induced variation of limiting factors. It is hoped that this research will facilitate a better understanding of the photosynthetic physiological mechanism by which potassium deficiency leads to growth retardation in oilseed rape.

Results

Plant performance, leaf K concentration and net photosynthesis. The total dry matter of the -K treatment decreased significantly by 29.9% on average versus the +K treatment (Table 1). The leaf expansion was also restrained, with a 22.1% and 18.0% decline in the individual leaf dry matter and leaf area, respectively. Leaf K concentration was dramatically influenced by potassium supply and leaf position, which was significantly lower in the -K treatment than in the +K treatment. Meanwhile, within an individual leaf, K concentration was remarkably lower in margins than in centers. The mean net photosynthesis (A) in the leaf margins of the -K treatment was 56.9% that of the +K treatment. However, there was no significant difference between leaf margins and centers under the -K treatment, as well as the two positions under the +K treatment.

Stomatal conductance. Potassium deficiency led to a significant decline of the mean stomatal conductance (g_s) in leaf margins, which was 63.6% that of the +K treatment. However, the mean g_s value of the leaf centers was not influenced by K nutrient (Table 2). There was a significantly lower g_s in leaf margins than in leaf centers under the -K treatment, whilst the g_s values of these two positions were the same under the +K treatment. Despite a

Treatment	Position	g_s (mol H ₂ O m ⁻² s ⁻¹)	C_i (μmol CO ₂ mol ⁻¹)	Stomatal frequency (no. mm ⁻²)	Stomatal length (μm)	Stomatal width (μm)	Single stomatal pore area (μm ²)	Total stomatal pore area (10 ⁻³ mm ² mm ⁻²)
-K	margin	0.142 ± 0.006b ¹	257 ± 6a	334.1 ± 7.0a	9.11 ± 0.07a	2.91 ± 0.02b	20.87 ± 0.15b	6.97 ± 0.05b
	center	0.231 ± 0.012a	240 ± 5a	334.7 ± 8.5a	9.94 ± 0.04a	3.49 ± 0.03a	27.30 ± 0.12a	9.14 ± 0.04a
+K	margin	0.223 ± 0.017a ²	238 ± 7a	335.7 ± 14.4a	10.01 ± 0.05a	3.68 ± 0.02a*	28.90 ± 0.14a*	9.70 ± 0.05a*
	center	0.238 ± 0.011a	231 ± 3a	338.5 ± 7.9a	10.66 ± 0.04a	3.54 ± 0.02a	29.64 ± 0.15a	10.03 ± 0.05a*

Table 2. Effects of K deficiency on stomatal conductance (g_s), intercellular CO₂ concentrations (C_i), stomatal frequency, length, and width, single stomatal pore area and total stomatal pore area of the two positions in the lower epidermis of the fifth fully expanded leaves. Images were taken at a magnification of × 500 with a scanning electron microscope. Values are mean ± SE of four replications for g_s , C_i , of 20 replications for stomatal frequencies, and of 300 replications for stomatal lengths, stomatal widths, stomatal pore areas and total stomatal pore areas. ¹Different letters in the same column at a given treatment indicate significant differences between positions ($P \leq 0.05$). ²*shows significant differences between the two K treatment in same position ($P \leq 0.05$).

Treatment	Position	g_m (mol CO ₂ m ⁻² s ⁻¹)	C_c (μmol CO ₂ mol ⁻¹)	C_i^* (μmol CO ₂ mol ⁻¹)	R_d (μmol CO ₂ m ⁻² s ⁻¹)	Γ^* (μmol CO ₂ mol ⁻¹)
-K	margin	0.084 ± 0.002b ¹	139 ± 3a	36.2 ± 0.8a	0.95 ± 0.03a	46.5 ± 1.6a
	center	0.151 ± 0.008a	132 ± 5b	35.4 ± 0.9a	0.92 ± 0.03a	41.7 ± 2.1a
+K	margin	0.163 ± 0.003a ²	127 ± 2a*	33.5 ± 1.4a	0.89 ± 0.05a	40.1 ± 1.5a*
	center	0.174 ± 0.018a	130 ± 7a	32.4 ± 1.7a	0.87 ± 0.04a	39.4 ± 2.0a

Table 3. Effects of K deficiency on mesophyll conductance (g_m), chloroplastic CO₂ concentrations (C_c), intercellular CO₂ compensation point (C_i^*), mitochondrial respiration rate in the light (R_d), and chloroplastic CO₂ compensation point (Γ^*) in the two positions of the fifth fully expanded leaves. C_i^* and R_d were measured by Laisk method, Γ^* was calculated according to the equation $\Gamma^* = C_i^* + R_d/g_m$. Values are mean ± SE of four replications for g_m , C_c , and $C_i - C_c$, of three replications for C_i^* , R_d and Γ^* . ¹Different letters in the same column at a given treatment indicate significant differences between positions ($P \leq 0.05$). ²*shows significant differences between the two K treatment in same position ($P \leq 0.05$).

decrease of the g_s value in leaf margins of the -K treatment, the intercellular CO₂ concentrations (C_i) value was raised, and the mean C_i were similar to those of other groups.

Potassium supply and leaf position had no effects on stomatal frequency and stomatal length (Table 2). However, stomatal width was significantly decreased in the -K treatment, especially in the leaf margins where the width decreased by 20.9% as compared with the +K treatment. Stomatal pore area was therefore considerably decreased due to K deficiency, particularly in the leaf margins with a 28.0% decline in the single stomatal pore area. Nevertheless, the stomatal length and width as well as the stomatal pore area showed no significant difference in these two positions under the +K treatment.

Mesophyll conductance. Despite a dramatic decrease in the mean mesophyll conductance (g_m) in the leaf margins of the -K treatment, the mean chloroplastic CO₂ concentrations (C_c) was 9.4% higher than that of the +K treatment (Table 3). The mean g_m and C_c values were similar in the leaf centers of different K treatments, as well as between the two positions in the +K treatment. Potassium nutrient and leaf position did not affect mean intercellular CO₂ compensation point (C_i^*) and mitochondrial respiration rate in the light (R_d), however, the mean chloroplastic CO₂ compensation point (Γ^*) was significantly increased in leaf margins of the -K treatment, but showed no statistical differences among the other three groups.

Biochemical characteristics. The mean maximum rate of electron transport (J_{max}) and maximum rate of carboxylation ($V_{c,max}$) in the leaf margins of the -K treatment were the lowest, and minor changes were observed among the other three treatments (Table 4). However, the mean $J_{max}/V_{c,max}$ in leaf margins of the -K treatment was dramatically increased compared with the mean values of the other three groups in the range from 1.42 to 1.46. The variation of photosynthetic parameters was verified by chemical analyses (Table 4). A significant decline of leaf chlorophyll concentration was found in the -K treated leaves, especially in the leaf margins, with a 31.1% decrease. Furthermore, Rubisco activity was dramatically decreased in leaf margins of the -K treatment, but it was the same in the leaf centers of the -K treatment and the two positions of the +K treatment. Potassium deficiency caused severe ROS production in leaf margins where O₂⁻ generation rate increased by 22.8%, and meanwhile, POD activity increased by 25.5%.

The relationship between relative A, g_s and g_m with leaf K concentration. A significant curvilinear relationship between relative A, g_s or g_m and leaf K concentrations is shown in Fig. 1. The relative values increased with increasing leaf K concentration, and remained stable when the leaf K concentration was beyond a certain concentration. Here a photosynthesis-based concentration threshold with the relative values reaching 95.0% of

Treatment	Position	J_{\max} ($\mu\text{mol m}^{-2}\text{s}^{-1}$)	$V_{c,\max}$ ($\mu\text{mol m}^{-2}\text{s}^{-1}$)	$J_{\max}/V_{c,\max}$	Chlorophyll (g m^{-2})	Rubisco activity ($\text{U g}^{-1}\text{FW}$)	O_2^- generation rate ($\text{nmol g}^{-1}\text{FW min}^{-1}$)	POD activity ($\text{U g}^{-1}\text{FW min}^{-1}$)
-K	margin	114.5 ± 9b ¹	70.9 ± 4.8b	1.61 ± 0.12a	0.42 ± 0.03b	0.29 ± 0.02b	8.77 ± 0.35a	2868 ± 176a
	center	166.2 ± 10a	113.9 ± 4.5a	1.46 ± 0.03b	0.54 ± 0.02a	0.36 ± 0.01a	6.97 ± 0.15b	2511 ± 74b
+K	margin	170.6 ± 12a*	120.5 ± 5.9a*	1.42 ± 0.06a*	0.61 ± 0.05a*	0.33 ± 0.01a*	7.18 ± 0.22a*	2275 ± 111a*
	center	167.5 ± 9a	118.0 ± 5.6a	1.42 ± 0.13a	0.64 ± 0.04a*	0.35 ± 0.01a	6.61 ± 0.33a	2085 ± 148a*

Table 4. Effects of K deficiency on the maximum rate of electron transport (J_{\max}), maximum rate of carboxylation ($V_{c,\max}$), ratio between J_{\max} and $V_{c,\max}$ ($J_{\max}/V_{c,\max}$) estimated from $A-C_c$ curves, chlorophyll concentration, Rubisco activity, O_2^- generation rate, and POD activity in the two positions of the fifth fully expanded leaves. Values are mean ± SE of four replications. ¹Different letters in the same column at a given treatment indicate significant differences between positions ($P \leq 0.05$). * shows significant differences between the two K treatment in same position ($P \leq 0.05$).

the maxima was defined. The relative A values increased rapidly with increasing leaf K concentration when it was less than 1.07% (Fig. 1a), and varied little when the leaf K concentration was above 1.07%. Therefore, the K concentration (1.07%) was used to evaluate the relative g_s and g_m (Fig. 1b,c), and the calculated result (93.7% and 94.3%) was close to 95.0%, indicating that this threshold value was acceptable for g_s and g_m .

Quantitative limitation analysis. The restrictions of A_{\max} in the -K leaves posed by stomatal (S_L), mesophyll conductance (MC_L) and biochemical limitations (B_L) are presented in Fig. 2a. In symptomatic margins, total limitations reached a value of 46.9%, and the contribution of S_L , MC_L and B_L represented 23.9%, 33.0% and 43.1% of total limitations, respectively. By contrast, despite the relatively low limitation (4.8%) in the leaf center, MC_L contributed a primary limitation to A_{\max} . Accordingly, the dominant limitations changed from symptomatic leaf margins to centers. The relationship between relative limitations and leaf K concentrations were further analyzed (Fig. 2b). All the limitations declined precipitously with the leaf K concentration increased from 0.6 to 1.07% (according to the K-based concentration threshold), particularly the B_L with the maximum slope of the fitted curve, but they gradually decrease as leaf K concentration continues to increase. Their relative contribution also varied with the change of the leaf K status. While MC_L largely predominated at the leaf K concentration of less than 1.07%, B_L replaced it when the K concentration was below 0.78% (leaf K concentration of the intersection point between B_L and MC_L fitted curves).

Discussion

Limitations imposed by K deficiency occur at the same time. In the present study, A in leaf margins were weakened by K deficiency. Generally, the declining A is considered to be limited by stomatal and mesophyll resistances to CO_2 diffusion, and biochemical obstacles^{13,22}. Here we demonstrated that g_s , g_m and biochemical activities were profoundly restricted as A down-regulated. Stomatal conductance which determine the vital step of CO_2 diffuse from the atmosphere to the interior of leaf was markedly decreased in -K leaf margins, as reported for *Eucalyptus grandis*¹, *Gossypium hirsutum*¹⁷, and *Oryza sativa*³. This is mainly because the lack of vacuole K to keep stomatal aperture by providing driving force to promote water inpour into the guard cell vacuole³¹. The declined A , to a certain extent, revealed that the K in cytoplasm identified as biochemical functional component was below the critical value¹⁰. Therefore, malfunction of physiological process could come with limited A .

Likewise, g_m was decreased in parallel with A . Indeed, g_m might be down-regulated by increasing leaf dry mass per area (M_A)^{7,23}, however, in the present study, there was no remarkable difference in M_A between the -K and +K leaves (Table 5; Supplementary Fig. S1). Cell wall thickness ($T_{\text{cell-wall}}$) and surface area of chloroplasts exposed to intercellular airspaces (S_c/S) are reported to be the most substantial anatomical traits in determining g_m ^{23,32}. However, significant differences in mesophyll cell wall surface area exposed to intercellular airspace per leaf area (S_m/S) and S_c/S , but not $T_{\text{cell-wall}}$ between leaf margins of two K treatments were observed (Table 5). Besides, chloroplast size³³ has also been proved to influence g_m . In the present study, though the chloroplast length (L_{chl}) decreased under lowest K status, the thickness (T_{chl}), surface area (S_{chl}) and volume (V_{chl}) of chloroplast were largely increased, however, the $S_{\text{chl}}/V_{\text{chl}}$ was smaller (Fig. 3). The chloroplast enlarging under lowest K concentration was not completely same to that discovered under low nitrogen conditions^{33,34}. The increase of T_{chl} was more likely to be based on the sacrifice of length owing to roughly circular envelope (Fig. 3a,b; Supplementary Fig. S2). Mathematically, ellipsoidal chloroplasts, combining with an increscent chloroplast number (see Supplementary Fig. S3) were more probably to have longer length of chloroplasts facing the cell wall than swollen even sphere envelopes. Furthermore, the resistance along diffusion pathway length in cytoplasm (distance of chloroplast from cell wall, $D_{\text{chl-cw}}$) and stroma (taken as half of the chloroplast thickness) account for 10–50% of g_m limitation²³, which however, reported only up to 22% of liquid phase resistance (r_{liq}) by Evans *et al.* in 1994³⁵. Low K status strongly increased T_{chl} and $D_{\text{chl-cw}}$ (Fig. 3b,f), accordingly, the corresponding resistance would be increased. It is therefore proved that the decreased g_m is primary due to the reduced S_c/S and larger cytosol diffusion resistance but not $T_{\text{cell-wall}}$. More evidences may seek from the influence of K on plasma membrane and chloroplast envelope conductance³², carbonic anhydrase and aquaporins that participated in determination of g_m ^{14,15,23}.

It should be noted that A , g_s or g_m started to decline almost at the same time with an extremely similar leaf K status. By another way, the quantitative analysis of limitations indicated that three limiting factors coexist when K concentration below 1.07%. This was similar to the results reported by Grassi and Magnani²² and Tezara *et al.*³⁶

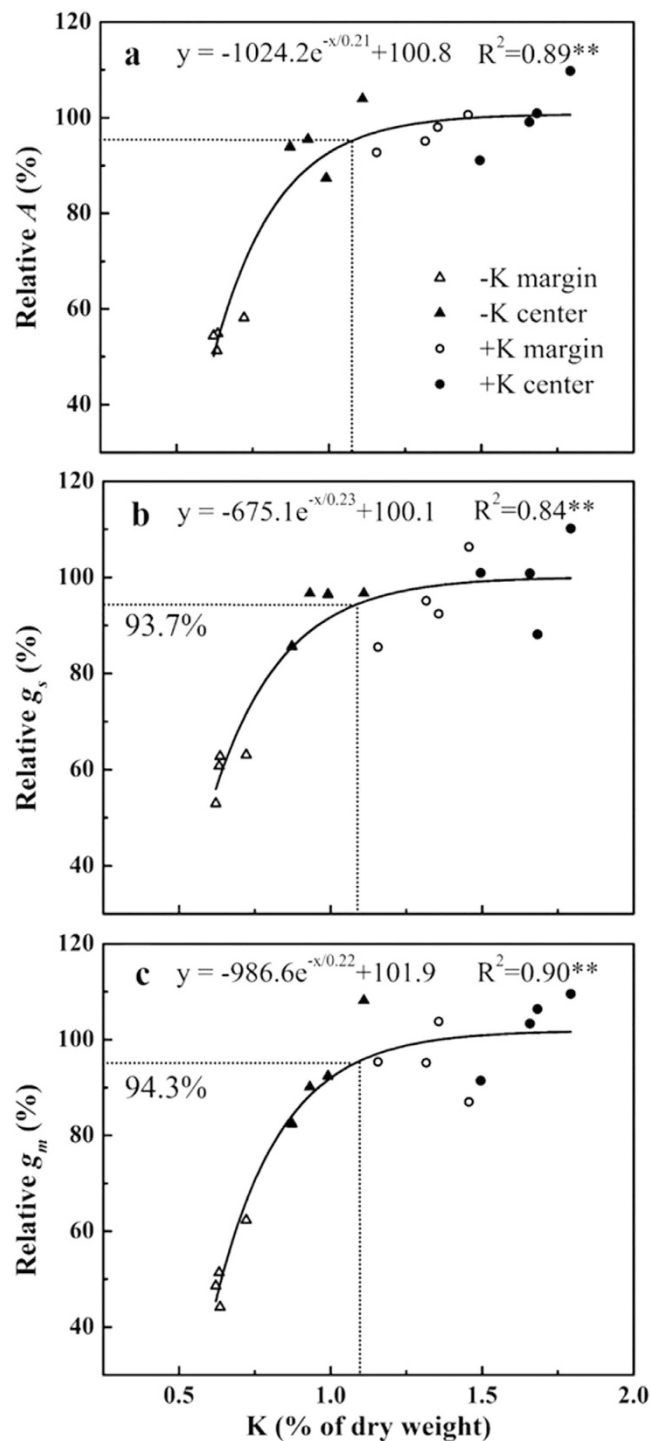


Figure 1. Relationship between relative photosynthetic parameters and leaf K concentration. Relative (a) photosynthesis rate (A), (b) stomatal conductance (g_s), (c) mesophyll conductance (g_m). The values were the relative proportion of measured values over the mean values of K-sufficient leaf centers. Each point represents one leaf measurement. Open triangles and closed triangles represent the values of leaf margin and leaf center under the $-K$ treatment, while open circles and closed circles represent those of the $+K$ treatment. Equations, regression coefficients, and significance are shown when $P \leq 0.05$ ($*P \leq 0.05$; $**P \leq 0.01$).

in plants suffering from water stress. However, the investigation carried out by Galmés *et al.*¹³ revealed that B_L of *Hypericum balearicum* and *Phlomis italica* still remained zero under mild water stress even if the total limitation reached 20–30%. The present finding highlights that all photosynthetic limitations simultaneously occur when leaf is in a physiological K-deficiency state.

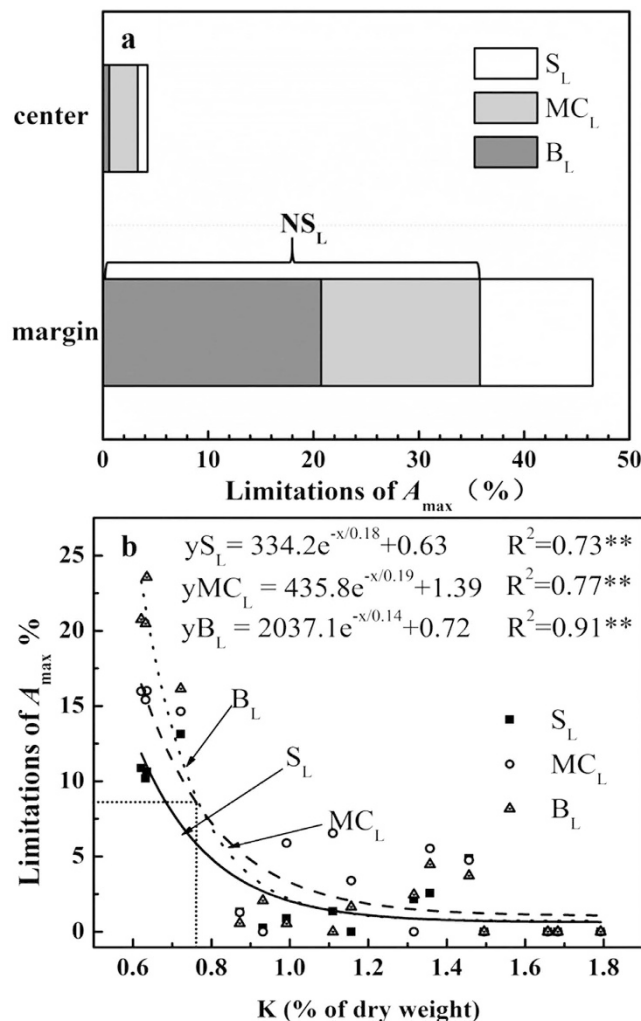


Figure 2. Photosynthetic limitations and their response to leaf K concentration. (a) Quantitative limitation analysis of photosynthetic CO₂ assimilation in leaf margins and centers under the -K treatment. Values are mean ± SE of four replicates per position. The open, gray, and dark gray bars represent the percentages of stomatal (S_L), mesophyll conductance (MC_L), and biochemical (B_L) limitations, respectively. (b) Relationships between limitations and leaf K concentration. Each point with the same shape represents a single leaf (n = 16). The symbols are as follows: S_L, closed squares; MC_L, open circles; B_L, closed triangles. Solid, dash, and dot lines are regression curves of S_L, MC_L, and B_L, respectively. Equations, regression coefficients, and significance are shown when $P \leq 0.05$ (* $P \leq 0.05$; ** $P \leq 0.01$).

Treatment	Position	T_{leaf} (μm)	$T_{cell-wall}$ (μm)	S_m/S (m ² m ⁻²)	S_c/S (m ² m ⁻²)
-K	margin	305 ± 27.7a	0.167 ± 0.017a	12.9 ± 1.8b	8.6 ± 1.1b
	center	310 ± 19.2a	0.170 ± 0.033a	17.1 ± 2.4a	12.8 ± 0.9a
+K	margin	309 ± 31.3a	0.172 ± 0.049a	17.4 ± 3.3a ²	13.1 ± 1.6a*
	center	312 ± 22.0a	0.176 ± 0.045a	18.2 ± 2.6a	13.5 ± 2.1a

Table 5. Effects of K deficiency on leaf thickness (T_{leaf}), mesophyll cell wall thickness ($T_{cell-wall}$), mesophyll cell wall surface area exposed to intercellular airspace per leaf area (S_m/S), and surface area of chloroplasts exposed to intercellular airspaces (S_c/S) in the two positions of the fifth fully expanded leaves. Data are mean ± SE of eight replications for S_m/S and S_c/S , at least thirty replications for T_{leaf} and $T_{cell-wall}$. ¹Different letters in the same column at a given treatment indicate significant differences between positions ($p \leq 0.05$). ²* shows significant differences between the two K treatment in same position ($p \leq 0.05$).

Limitations vary with increasing K deficiency intensity. The leaf K concentration threshold value observed in this study was 1.07%, in consistent with the range of 0.5 to 2.0% reported by Leigh and Wyn Jones³⁷. Quantitative limitation analysis gives insight into the contributions of different photosynthetic limitations, revealing that the B_L and MC_L accounted for the majority of total limitations in K-starved leaf margins and

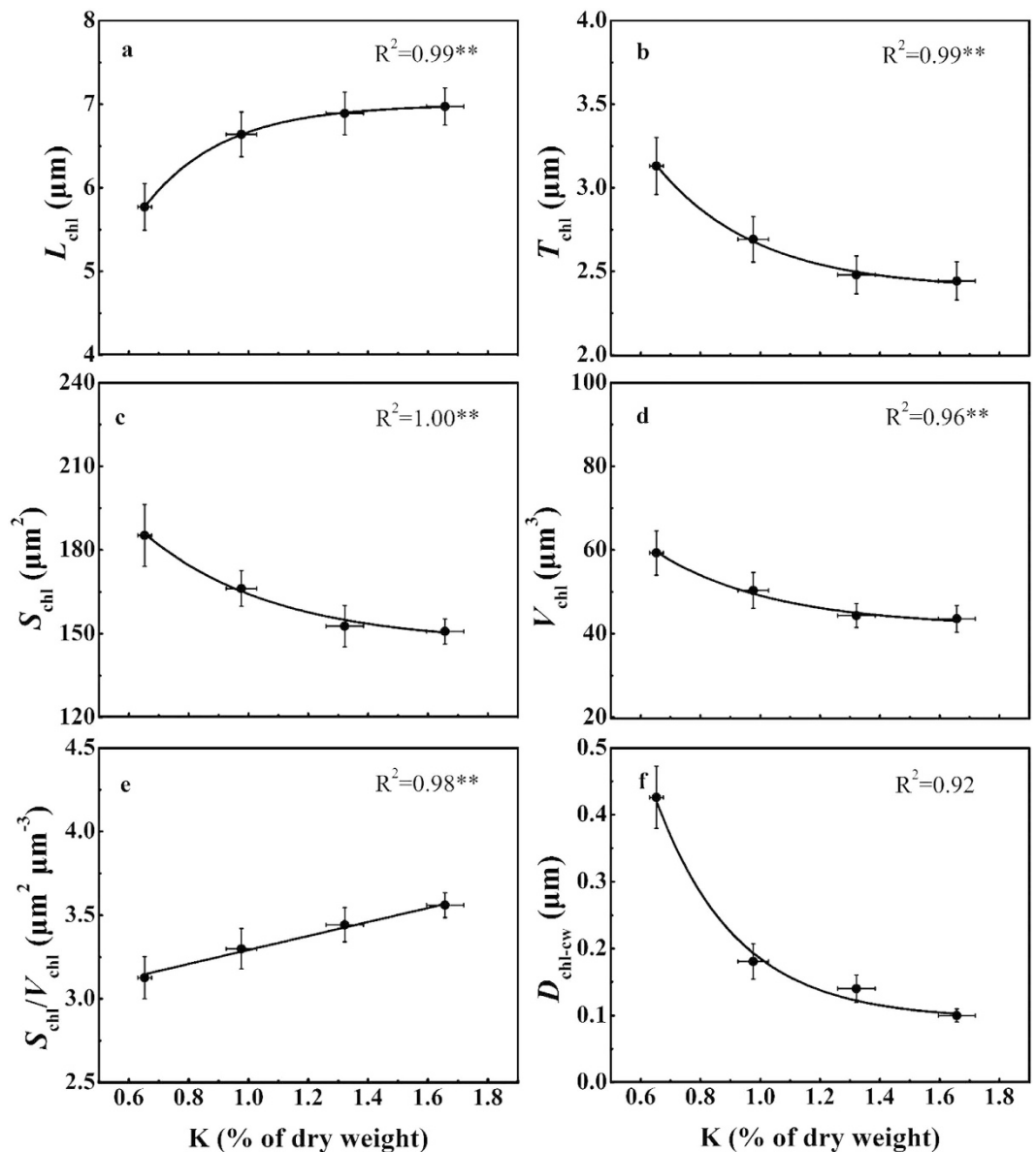


Figure 3. The relationship between chloroplast characteristics and leaf K concentration. (a) Chloroplast length (L_{chl}), (b) thickness (T_{chl}), (c) surface area (S_{chl}), (d) volume (V_{chl}), (e) S_{chl}/V_{chl} , (f) distance of chloroplast from the cell wall (D_{chl-cw}). Values are mean \pm SE of four replicates for K concentration and at least thirty replicates for microstructure parameters. Regression coefficients and significance are shown when $P \leq 0.05$ (* $P \leq 0.05$; ** $P \leq 0.01$).

centers, respectively. This is mainly ascribed to the discrepancy of relative severity of K deficiency^{5,6}. As has been stated in the previous studies that some irreversible damages, such as impaired ATP synthesis, depressed Rubisco activity, and cell damage occurred when the limiting A , for the most part, is attributed to B_L ^{3,38}. Some of which were verified in the present study, such as degraded chloroplast, limited photoassimilate transportation (see Supplementary Fig. S2), and increased O_2^- generation rate under severe K deficiency. The obstacle of these physiological processes alleviated as K deficient stress mitigating, however, the role of MC_L on A began to stand out.

The relationship between relative limitations and leaf K concentration verified that, at a leaf K concentration of less than 1.07%, MC_L represented the main component of limitations, but B_L replaced it when leaf K concentration below 0.78%. This pattern, to a lesser extent, could be found in plants suffering from water stress which suggested that the variation of limitations depends on the stress intensity and duration²². Regrettably, the present study failed to reveal whether or not there is a critical concentration in the shifting process from S_L predominance to MC_L predominance. Further studies focusing on the photosynthetic limitations of rapeseed leaves subjected to a serial K gradient may help to elucidate this issue.

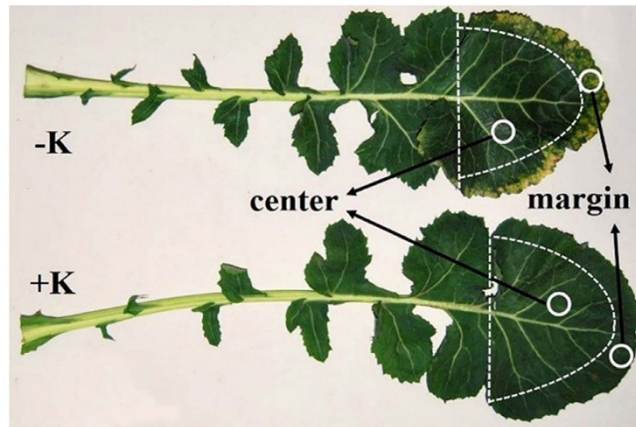


Figure 4. Leaves under the -K and +K treatments. The vertical dash lines divide leaf into two parts, the leaf apices are separated into leaf margins and leaf centers by half-elliptical lines. White circles indicate the gas exchange measuring positions.

Methods

Study site and growth conditions. A field experiment was conducted in Wuxue county, Hubei province, central China (30° 06' 46" N, 115° 36' 9" E) during the 2013–2014 oilseed rape growing season. The mean temperature of the season was 13.8 °C, and the average temperature during winter (from December 2013 to February 2014) was 5.9 °C. The total precipitation during oilseed rape cropping season was 660.7 mm, with wintertide accounting for 26.1% of the total. The soil was a sandy loam with pH 5.3, organic matter 30.5 g kg⁻¹, total N 1.7 g kg⁻¹, NH₄OAc-K 42.5 mg kg⁻¹, Olsen-P 15.7 mg kg⁻¹ and hot-water soluble B 0.78 mg kg⁻¹ in the topsoil layer (0–20 cm). As stated by Zou, the soil belongs to a K-deficient type, which would cause yield reduction without K fertilizer addition⁴.

Experimental design. A complete randomized block design was set up with two treatments and four replicates. The treatments were: (1) Sufficient K supply treatment (+K), with a K fertilizer recommendation rate of 120 kg K₂O ha⁻¹ which was tested and well-proved to ensure the optimal growth and yield formation of oilseed rape based on field experiments in this region³⁹. (2) K deficiency treatment (-K), with no K fertilizer applied throughout the growing season.

To ensure that nutrients other than K did not limit plant K uptake, 180 kg N ha⁻¹, 90 kg P₂O₅ ha⁻¹, and 1.6 kg B ha⁻¹ were applied for these two treatments. The N, P, K, B fertilizers used in the experiment consisted of urea (46% N), superphosphate (12% P₂O₅), potassium chloride (60% K₂O), and borax (10.8% B). The N fertilizer was applied in three splits: 60% prior to transplanting, i.e., BBCH (Biologische Bundesanstalt, Bundessortenamt and Chemische Industrie) 15–16⁴⁰, 20% at the over-wintering stage (i.e., BBCH 29), and 20% at the initiation of stem elongation (i.e., BBCH 30). Besides, all the P, K, B fertilizers were applied as basal fertilizers. The experimental field was plowed and leveled with a rotary tiller, and basal fertilizers were incorporated during the process. The plot measured 20 m² with a length of 10 m and a width of 2 m.

The oilseed rape cultivar was Zhongshuang 11, supplied by Oil Crops Research Institute of the Chinese Academy of Agricultural Sciences. Rapeseeds were sown in prepared seedbeds on 16 September 2013, and then, on 22 October, about 36 d after sowing, oilseed-rape seedlings with five to six leaves (i.e., BBCH 15–16, 3–4 g dry weight plant⁻¹) were uniformly selected and transplanted by hand in double rows spaced approximately 0.3 m apart with 0.2–0.3 m between plants, corresponding to 112 500 plants ha⁻¹. The oilseed rape was grown under rain-fed conditions. Meanwhile, weeds, pests and disease stresses were controlled by spray herbicides, insecticide and fungicide so that no obvious weeds, insect pests, and diseases infestation occurred during cropping season.

Plant and leaf tagging. There was an obvious phenotypic difference in plants between the -K and +K treatments 60 d after transplanting. The discrepancy was highlighted in the fifth to ninth fully expanded leaves (with a total average of 9 fully expanded leaves (i.e., BBCH 19) in both treatments) from apex downwards, specifically, obvious etiolation symptoms around the periphery in K-deficient leaves and asymptomatic leaves in the +K treatment. For each treatment, 24 fifth fully expanded leaves and six uniform plants were tagged in each of the four replicate plots for destructive and non-destructive analysis described later in the methods.

Leaf gas exchange and fluorescence measurements. Leaf gas exchange and chlorophyll fluorescence were measured simultaneously at either leaf margins (Fig. 4, about 2 cm of leaf surface from the margin) or leaf centers (the rest part between half-elliptical and vertical dashed lines), using a portable, open circuit, infrared gas analysis system (Li-6400, Li-Cor Inc., Lincoln, NE, USA) equipped with an integrated leaf chamber fluorometer (Li-6400-40). Measurements were performed on at least four randomly selected leaves of both treatments in the late morning (11:00–12:30) under a light-saturating photosynthetic photon flux density (PPFD) of 1200 μmol m⁻²s⁻¹ (with 90% red light and 10% blue light). CO₂ concentration in the leaf chamber (C_a) was set at 400 μmol mol⁻¹ air, leaf temperature was controlled at 25 ± 0.2 °C, relative humidity was between 50 and 60%, and the flow rate was 500 μmol s⁻¹. In addition to net photosynthesis (A), stomatal conductance to water vapour (g_s) and intercellular

CO₂ concentration (C_i), the incorporated fluorometer allowed determination the steady-state fluorescence yield (F_s) under actinic light and maximum fluorescence (F'_m) during light-saturating pulse (0.8 s) of approx. 8000 $\mu\text{mol m}^{-2} \text{s}^{-1}$. The relative A , g_m and g_m values were the relative proportion of measured values over the mean values of K-sufficient leaf centers.

A/C_i curves were measured on the two positions that had been previously acclimated to saturating light conditions for 20 min. The CO₂ concentration (C_a) in the gas exchange chamber was reduced stepwise from 400 to 300, 250, 200, 150, 100, 50 $\mu\text{mol CO}_2 \text{ mol}^{-1}$, and then increased from 50 to 400, 600, 800, 1000, 1200, 1500, 1800 $\mu\text{mol CO}_2 \text{ mol}^{-1}$ at a constant PPFD of 1200 $\mu\text{mol m}^{-2} \text{s}^{-1}$ at $25 \pm 0.2^\circ\text{C}$, and 50–60% relative humidity. In all cases, the parameters were recorded after the gas exchange rate stabilized at the given C_a . At least four leaves were performed in each treatment.

The actual photochemical efficiency of photosystem II (Φ_{PSII}) was then determined as follows⁴¹:

$$\Phi_{\text{PSII}} = \frac{F'_m - F_s}{F'_m} \quad (1)$$

The electron transport rate (J) can be calculated as:

$$J = \Phi_{\text{PSII}} \times \text{PPFD} \times \alpha \times \beta \quad (2)$$

Where α is the leaf absorptance, and β is the fraction of light distributed to PSII. As routinely assumed, α was taken as 0.85^{42,43} and β was taken as 0.5^{44,45}. A sensitivity analysis of J biases resulting from rough assumption of α and β on g_m variations was also conducted (See Supplementary Table S5).

Mesophyll conductance was estimated according to Harley *et al.* from combined gas exchange and chlorophyll fluorescence measurements⁴⁶.

$$g_m = \frac{A}{C_i - \frac{\Gamma^*(J + 8(A + R_d))}{J - 4(A + R_d)}} \quad (3)$$

where A , C_i and J were determined as previously described for each treatment, mitochondrial respiration rate in the light (R_d) and the intercellular CO₂ compensation point (C_i^*) were measured by Laisk method, as described by Brooks and Farquhar⁴⁷. Briefly, the A/C_i curves generated with PPFD values of 75, 150, 500 $\mu\text{mol m}^{-2} \text{s}^{-1}$, respectively, with each having five different C_a in chamber (i.e. 50, 80, 100, 120 and 150 $\mu\text{mol CO}_2 \text{ mol}^{-1}$). A linear regression was then fitted to each A/C_i curve. The x -axis and y -axis of intersection point of three A/C_i curves were defined as C_i^* and R_d ⁴⁸. The Γ^* is the chloroplastic CO₂ photocompensation point calculated from C_i^* and R_d as:

$$\Gamma^* = C_i^* + \frac{R_d}{g_m} \quad (4)$$

For each data point generated, we checked whether it met the range of $10 < dC_c/dA < 50$ ⁴⁶. The CO₂ concentration in the chloroplast stroma (C_c) was calculated as:

$$C_c = C_i + \frac{A}{g_m} \quad (5)$$

Therefore, $A-C_i$ curves were converted into $A-C_c$ curves. On the basis of C_c , the maximum rate of Rubisco-catalysed carboxylation ($V_{c,\text{max}}$), and the maximum rate of electron transport (J_{max}) as defined by Farquhar *et al.*⁴⁹, were calculated^{11,50}.

Since variable J method is sensitive to many sources of errors, e.g. (1) Γ^* and R_d biases; (2) a wrong assumption of p_1 and p_2 ; (3) biases in the measurements of C_i , A , and J , a sensitivity analysis would be great values to improve the confidence in g_m estimates and following limitation calculations⁵¹. Following the method of Harley *et al.*⁴⁶, we used actual Γ^* , R_d and J values calculated in this study and a deviation from the measured values to analyze the effects of Γ^* , R_d and J on g_m estimates (see Supplementary Table S1, S3, S5). RuBP regeneration can be limited by either insufficient NADPH or ATP, according to Farquhar model, A and J can be linked as follows:

$$A = \frac{J(C_c - \Gamma^*)}{p_1 C_c + p_2 \Gamma^*} - R_d \quad (6)$$

For insufficient NADPH, $p_1 = 4$ and $p_2 = 8$; for insufficient ATP, $p_1 = 4.5$ and $p_2 = 10.5$ or $p_1 = 4$ and $p_2 = 9.33$. Finally, the sensitivity analysis for photosynthetic limitations was conducted basing on these calculated g_m values (see Supplementary Table S2, S4, S6). The analysis showed that the g_m was significantly affected by varying Γ^* and R_d (see Supplementary Table S1), p_1 and p_2 inputs (see Supplementary Table S3) and J biases (see Supplementary Table S5). However, the g_m variation derived from Γ^* , R_d , J , p_1 and p_2 biases, did not cause profound effects on photosynthetic limitations (see Supplementary Table S2, S4, S6). In addition, g_m appears to be strikingly affected by C_i ^{12,14,51}, nevertheless, the similar C_i in different treatments and positions here seems to have no impact on g_m (Table 3). Therefore, the results obtained was unlikely to be altered by these methodological artifacts.

Plant dry matter, leaf area and dry matter. Six tagged leaves and six tagged plants in each plot were used to determine the individual leaf area, dry matter, and total dry matter. Each leaf was digitally scanned using an Epson ES-1200C scanner (Epson, Long Beach, CA, USA), and the area determined using ImageJ software

(National Institutes of Health, Bethesda, Maryland, USA)¹. Individual leaf dry matter and total dry matter were weighed after oven drying at 65 °C for 48 h.

Biochemical analysis. Twelve tagged leaves per plot were picked immediately after the determination of photosynthesis. They were divided into two parts along vertical dashed lines (Fig. 4), followed by dissecting the leaf apices into leaf margins and leaf centers, and removing all the veins. A portion of segments were immersed in liquid N and then stored at −78 °C, and the rest were used for leaf K concentration determination. There were four replications for biochemical determinations.

Leaf segments (2 g) were oven dried at 65 °C for 48 h. After that, about 0.15 g dried leaves were milled and digested with H₂SO₄-H₂O₂ as described by Thomas *et al.*⁵², and K concentration in digestion solution was measured by a flame photometer (M-410, Cole-Parmer, Chicago, IL, USA).

The Rubisco extracts were prepared according to Weng *et al.* with minor modifications³. Briefly, leaf segments (0.2 g) were ground to a powder using a chilled mortar and pestle with liquid N₂ and a small amount of quartzsand, followed by homogenization with 4 mL pre-cooled extraction buffer containing 50 mM Tris-HCl (pH 7.5), 1 mM EDTA, 10 mM MgCl₂, 12.5% (v/v) glycerol, 10 mM (v/v) β-mercaptoethanol and 1% (w/v) PVP-40 (soluble PVP) at 0–4 °C. The homogenate was centrifuged for 15 min at 15 000 g at 4 °C, and then the supernatant was immediately used to determine the activity of ribulose-1, 5-bisphosphate carboxylase/oxygenase (Rubisco, EC 4.1.1.39) by an enzyme-linked immunosorbent assay method with a RuBPCase ELISA kit (CK-E91697P, Shanghai jijin Chemistry and Technology Co., Ltd, China) according to the manufacturer's instructions. The chlorophyll concentration was determined according to the method of Huang *et al.*⁵³.

Superoxide radical O₂^{•−} production rate was measured by monitoring the nitrite formation from hydroxylamine in the presence of O₂^{•−} according to Elstner and Heupel⁵⁴. A 0.5 g aliquot of leaf margins and centers was ground and homogenized in 5 mL of 65 mM pre-cooled phosphate buffer (pH 7.8), followed by centrifuging the homogenate at 10,000 g for 15 min at 4 °C and mixing 0.5 mL of the supernatant with phosphate buffer (0.5 mL) and 0.1 mL of 10 mM hydroxylamine hydrochloride. This mixture was incubated at 25 °C for 20 min, followed by the addition of 1 mL of 58 mM sulfanilic acid and 1 mL of α-naphthylamine, and then another 20 min incubation at 25 °C. The as-prepared solution was shaken with equal volume of ether, followed by centrifuging the mixture at 10,000 g for 3 min and measuring the absorbance of the pink water phase at 530 nm. The activity of POD (EC 1.11.1.7) was determined using the guaiacol oxidation method⁵⁵.

Anatomical analysis. Another six tagged leaves per treatment were collected, and removed all the veins for anatomical analysis. The stomatal size and frequency were measured in six sub-samples either for leaf margin or center. The materials were prepared as described by Meng *et al.*⁵⁶. Briefly, leaf samples (about 1 cm in length and 1 cm in width) were fixed in 2.5% glutaraldehyde (v/v) at 4 °C for 2 h, and washed twice in 0.1 M phosphate buffer (pH 6.8). Next, they were sequentially dehydrated in ethanol (30%, 50%, 70%, 80%, 90%, 95%, and 100%) for 10 min at each gradient concentration, with 100% ethanol repeated twice. After further drying and spraying with gold, the as-treated leaf samples were observed and photographed with a scanning electron microscope (JSM-5310LV, Jeol Co, Tokyo, Japan). Images were taken of the lower leaf surface for five microscope fields per sub-sample at a magnification of ×500. The number of stomata was counted in each field (a total of 20 measurements of stomatal frequency for each position) as described by Battie-Laclau *et al.*¹, and the stomatal frequency was calculated by dividing the stomatal count by the area of the field of view⁵⁷. Moreover, the length and width of ten stomata selected at random were measured in each field. Assuming the stomatal pore as an ellipse, the total stomatal pore area was calculated (stomatal frequency × π × 0.25 × stomatal length × stomatal width).

Leaf segments (1–2 mm²) were cut from each part and fixed with 2.5% glutaraldehyde (v/v) in 0.1 M phosphate buffer (pH 7.4) for 4 h, followed by washing twice in the same buffer for 30 min and postfixing with 2% osmium tetroxide for 4 h at 4 °C. Next, the samples were dehydrated with an ethanol series (10–100%) and in propylene oxide, followed by embedding them in Epon 812 resin.

For the light microscope observation, they were cut into 1 μm transverse sections by LKB-5 ultramicrotome 359 (LKB Co., Ltd., Uppsala, Sweden), and stained with 0.5% toluidine blue. Micrographs were captured at a magnification of ×400 with a Nikon Eclipse E600 microscope equipped with a Nikon 5 MP digital microscope camera DS-Fi1 (Nikon Corporation, Kyoto, Japan). There were four samples per treatment. For each samples, three cross-sections were chosen to measure their thickness (*T*_{leaf}), mesophyll cell wall surface area exposed to intercellular airspace per leaf area (*S*_{mes}/*S*), and surface area of chloroplasts exposed to intercellular airspaces (*S*_c/*S*) according to Tosens *et al.* (2012)³².

$$S_{\text{mes}}/S = \frac{L_{\text{mes}}}{W} \times F \quad (7)$$

$$S_c/S = \frac{L_c}{L_{\text{mes}}} \times S_{\text{mes}}/S \quad (8)$$

Where *L*_{mes} and *L*_c are the length of mesophyll cell wall exposing to intercellular air space and chloroplast surface area touching the intercellular air space. *W* is the width of measured cross-section. *F* is the curvature correction factor which was obtained as the weight average of palisade and spongy mesophyll.

For the ultrastructural observations, ultrathin sections (90 nm) were examined with a transmission electron microscope (H-7650, Hitachi, Japan) after staining with 2.0% uranyl acetate (w/v) and lead citrate. Cell wall thickness (*T*_{cell-wall}), chloroplast length (*L*_{chl}) and thickness (*T*_{chl}) were measured from at least 30 chloroplasts. Chloroplasts were assumed as ellipsoids, and chloroplast surface area (*S*_{chl}) and volume (*V*_{chl}) were calculated according Cesaro formula⁵⁸:

$$S_{\text{chl}} = 4 \times \pi \times \sqrt[3]{(a \times b^2)^2} \quad (9)$$

$$V_{\text{chl}} = \frac{4}{3} \times \pi \times a \times b^2 \quad (10)$$

where $a = 0.5 \times L_{\text{chl}}$; $b = 0.5 \times T_{\text{chl}}$. Distance of chloroplast from cell wall ($D_{\text{chl-cw}}$) was determined according to Tomás *et al.*²³.

Quantitative limitation analysis. The limitations (stomatal limitations, S_L ; mesophyll conductance limitations, MC_L ; biochemical limitations, B_L) imposed by K deficiency on photosynthesis were investigated by analyzing the leaf margins and centers under two treatments using the quantitative limitation analysis method proposed by Grassi and Magnani²². Relative changes in light-saturated assimilation is expressed in terms of relative changes in stomatal, mesophyll conductance, and biochemical capacity as Equation (11).

$$\frac{dA}{A} = S_L + MC_L + B_L = l_s \cdot \frac{dg_{sc}}{g_{sc}} + l_{mc} \cdot \frac{dg_m}{g_m} + l_b \cdot \frac{dV_{c, \max}}{V_{c, \max}} \quad (11)$$

where l_s , l_{mc} , and l_b are the corresponding relative limitations calculated as Eqns from (12) to (14), g_{sc} is stomatal conductance to CO_2 ($g/1.6$), and $V_{c, \max}$ is maximum rate of carboxylation estimated from $A-C_i$ curve.

$$l_s = \frac{g_{\text{tot}}/g_{sc} \cdot \partial A/\partial C_c}{g_{\text{tot}} + \partial A/\partial C_c} \quad (12)$$

$$l_m = \frac{g_{\text{tot}}/g_m \cdot \partial A/\partial C_c}{g_{\text{tot}} + \partial A/\partial C_c} \quad (13)$$

$$l_b = \frac{g_{\text{tot}}}{g_{\text{tot}} + \partial A/\partial C_c} \quad (14)$$

where g_{tot} is the total conductance to CO_2 from leaf surface to carboxylation sites determined as Equation (15). By following Tomás *et al.*²³, $\partial A/\partial C_c$ was calculated as slope of $A-C_c$ response curves over a C_c range of 50–100 $\mu\text{mol mol}^{-1}$.

$$g_{\text{tot}} = \frac{1}{1/g_{sc} + 1/g_m} \quad (15)$$

Then the relative change of A , g_{sc} , g_m and $V_{c, \max}$ in Equation (11) can be approximated by Chen *et al.*⁵⁹.

$$\frac{dA}{A} \approx \frac{A_{\text{max}}^{\text{ref}} - A}{A_{\text{max}}^{\text{ref}}} \quad (16)$$

$$\frac{dg_{sc}}{g_{sc}} \approx \frac{g_{sc}^{\text{ref}} - g_{sc}}{g_{sc}^{\text{ref}}} \quad (17)$$

$$\frac{dg_m}{g_m} \approx \frac{g_m^{\text{ref}} - g_m}{g_m^{\text{ref}}} \quad (18)$$

$$\frac{dV_{c, \max}}{V_{c, \max}} \approx \frac{V_{c, \max}^{\text{ref}} - V_{c, \max}}{V_{c, \max}^{\text{ref}}} \quad (19)$$

where $A_{\text{max}}^{\text{ref}}$, g_{sc}^{ref} , g_m^{ref} and $V_{c, \max}^{\text{ref}}$ are the reference values of net CO_2 assimilation rate, stomatal conductance and mesophyll conductance, and the rate of carboxylation, defined as maximum value measured under light saturation. In the original reference, the authors used the maximum value of seasonal A_{max} under light-saturated conditions as a reference to assess the photosynthetic limitations of A for each determination. In the current study, the maximum A was generally reached, concomitantly with g_s , g_m and $V_{c, \max}$ in the leaf centers with the +K treatment, and the mean values of the +K treatments was thus used as a reference, i.e., there was no limitation present in the leaf centers under the +K treatment. Whenever one of the three parameters was higher in either one of the rest treatment than that of the reference, its corresponding limitation was set to zero. In this way, the limitations in the leaf margins and centers under the -K treatment could be quantified. Finally, non-stomatal limitations were defined as the sum of mesophyll conductance limitations and biochemical limitations ($NS_L = MC_L + B_L$).

Statistical analysis. One-way analysis of variance (ANOVA) was calculated using SPSS 18.0 software (SPSS, Chicago, IL, USA). The mean values were compared using the least significant difference (LSD) test ($P < 0.05$). Graphics and regression analysis were performed using the OriginPro 8.5 software (OriginLab Corporation, Northampton, MA, USA).

References

- Battie-Laclau, P. *et al.* Photosynthetic and anatomical responses of *Eucalyptus grandis* leaves to potassium and sodium supply in a field experiment. *Plant cell environ.* **37**, 70–81 (2014).
- Erel, R. *et al.* Modification of non-stomatal limitation and photoprotection due to K and Na nutrition of olive trees. *J. Plant physiol.* **177**, 1–10 (2015).
- Weng, X. Y., Zheng, C. J., Xu, H. X. & Sun, J. Y. Characteristics of photosynthesis and functions of the water-water cycle in rice (*Oryza sativa*) leaves in response to potassium deficiency. *Physiol. plantarum* **131**, 614–621 (2007).
- Zou, J., Lu, J. W., Li, Y. S. & Li, X. K. Regional evaluation of winter rapeseed response to K fertilization, K use efficiency, and critical level of soil K in the Yangtze River Valley. *Sci. Agric. Sin.* **10**, 911–920 (2011).
- Bednarz, C., Oosterhuis, D. & Evans, R. Leaf photosynthesis and carbon isotope discrimination of cotton in response to potassium deficiency. *Environ. Exp. Bot.* **39**, 131–139 (1998).
- Jin, S. H. *et al.* Effects of potassium supply on limitations of photosynthesis by mesophyll diffusion conductance in *Carya cathayensis*. *Tree physiol.* **31**, 1142–1151 (2011).
- Flexas, J., Ribas-Carbó, M., Diaz-Espejo, A., Galmés, J. & Medrano, H. Mesophyll conductance to CO₂: current knowledge and future prospects. *Plant Cell Environ.* **31**, 602–621 (2008).
- Lebaudy, A. *et al.* Plant adaptation to fluctuating environment and biomass production are strongly dependent on guard cell potassium channels. *P. Natl. Acad. Sci. USA* **105**, 5271–5276 (2008).
- Andrés, Z. *et al.* Control of vacuolar dynamics and regulation of stomatal aperture by tonoplast potassium uptake. *P. Natl. Acad. Sci. USA* **111**, 1806–1814 (2014).
- Jordan-Meille, L. & Pellerin, S. Shoot and root growth of hydroponic maize (*Zea mays* L.) as influenced by K deficiency. *Plant Soil* **304**, 157–168 (2008).
- Bernacchi, C. J., Portis, A. R., Nakano, H., von Caemmerer, S. & Long, S. P. Temperature response of mesophyll conductance. Implications for the determination of Rubisco enzyme kinetics and for limitations to photosynthesis *in vivo*. *Plant Physiol.* **130**, 1992–1998 (2002).
- Flexas, J. *et al.* Rapid variations of mesophyll conductance in response to changes in CO₂ concentration around leaves. *Plant Cell Environ.* **30**, 1284–1298 (2007).
- Galmés, J., Medrano, H. & Flexas, J. Photosynthetic limitations in response to water stress and recovery in Mediterranean plants with different growth forms. *New Phytol.* **175**, 81–93 (2007).
- Xiong, D. L. *et al.* Rapid responses of mesophyll conductance to changes of CO₂ concentration, temperature and irradiance are affected by N supplements in rice. *Plant Cell Environ.* doi: 10.1111/pce.12558 (2015).
- Kaldenhoff, R. Mechanisms underlying CO₂ diffusion in leaves. *Curr. Opin. Plant Biol.* **15**, 276–281 (2012).
- Kanai, S. *et al.* Potassium deficiency affects water status and photosynthetic rate of the vegetative sink in green house tomato prior to its effects on source activity. *Plant sci.* **180**, 368–374 (2011).
- Wang, N. *et al.* Genotypic variations in photosynthetic and physiological adjustment to potassium deficiency in cotton (*Gossypium hirsutum*). *J. Photochem. Photobiol. B: Biol.* **110**, 1–8 (2012).
- Niinemets, Ü. *et al.* Do we underestimate the importance of leaf size in plant economics? Disproportional scaling of support costs within the spectrum of leaf physiognomy. *Ann. Bot.* **100**, 283–303 (2007).
- Cakmak, I. The role of potassium in alleviating detrimental effects of abiotic stresses in plants. *J. Plant Nutr. Soil Sci.* **168**, 521–530 (2005).
- Paul, M. J. & Pellny, T. K. Carbon metabolite feedback regulation of leaf photosynthesis and development. *J. Exp. Bot.* **54**, 539–547 (2003).
- Araya, T., Noguchi, K. & Terashima, I. Effects of carbohydrate accumulation on photosynthesis differ between sink and source leaves of *Phaseolus vulgaris* L. *Plant cell physiol.* **47**, 644–652 (2006).
- Grassi, G. & Magnani, F. Stomatal, mesophyll conductance and biochemical limitations to photosynthesis as affected by drought and leaf ontogeny in ash and oak trees. *Plant Cell Environ.* **28**, 834–849 (2005).
- Tomás, M. *et al.* Importance of leaf anatomy in determining mesophyll diffusion conductance to CO₂ across species: quantitative limitations and scaling up by models. *J. Exp. Bot.* **64**, 2269–2281 (2013).
- Gago, J. *et al.* Photosynthesis limitations in three fern species. *Physiol. plantarum* **149**, 599–611 (2013).
- Muir, C. D., Hangarter, R. P., Moyle, L. C. & Davis, P. A. Morphological and anatomical determinants of mesophyll conductance in wild relatives of tomato (*Solanum* sect. *Lycopersicon*, sect. *Lycopersicoides*; Solanaceae). *Plant cell environ.* **37**, 1415–1426 (2014).
- Ren, T. *et al.* Potassium-fertilizer management in winter oilseed-rape production in China. *J. Plant Nutr. Soil Sci.* **176**, 429–440 (2013).
- Gierth, M. & Mäser, P. Potassium transporters in plants— involvement in K⁺ acquisition, redistribution and homeostasis. *FEBS lett.* **581**, 2348–2356 (2007).
- Gonzalez, N., Vanhaeren, H. & Inzé, D. Leaf size control: complex coordination of cell division and expansion. *Trends Plant Sci.* **17**, 332–340 (2012).
- Zörb, C., Senbayram, M. & Peiter, E. Potassium in agriculture—status and perspectives. *J. Plant Physiol.* **171**, 656–669 (2014).
- Fanaei, H., Galavi, M., Kafi, M. & Bonjar, A. G. Amelioration of water stress by potassium fertilizer in two oilseed species. *Int. J. Plant Prod.* **3**, 41–54 (2009).
- Peiter, E. The plant vacuole: emitter and receiver of calcium signals. *Cell Calcium* **50**, 120–128 (2011).
- Tosens, T., Niinemets, Ü., Westoby, M. & Wright, I. J. Anatomical basis of variation in mesophyll resistance in eastern Australian sclerophylls: news of a long and winding path. *J. Exp. Bot.* **63**, 5105–5119 (2012).
- Li, Y. *et al.* Does chloroplast size influence photosynthetic nitrogen use efficiency? *PLoS ONE* **8**, e62036 doi: 10.1371/journal.pone.0062036 (2013).
- Xiong, D. L. *et al.* SPAD-based leaf nitrogen estimation is impacted by environmental factors and crop leaf characteristics. *Scientific Reports* **5**, 13389 doi: 10.1038/srep13389 (2015).
- Evans, J. R., von Caemmerer, S., Setchell, B. A. & Hudson, G. S. The relationship between CO₂ transfer conductance and leaf anatomy in transgenic tobacco with a reduced content of Rubisco. *Aust. J. Plant Physiol.* **21**, 475–495 (1994).
- Tezara, W., Mitchell, V., Driscoll, S. & Lawlor, D. Effects of water deficit and its interaction with CO₂ supply on the biochemistry and physiology of photosynthesis in sunflower. *J. Exp. Bot.* **53**, 1781–1791 (2002).
- Leigh, R. A. & Wyn Jones, R. G. A hypothesis relating critical potassium concentrations for growth to the distribution and functions of this ion in the plant cell. *New Phytol.* **97**, 1–13 (1984).
- Flexas, J., Bota, J., Loreto, F., Cornic, G. & Sharkey, T. D. Diffusive and metabolic limitations to photosynthesis under drought and salinity in C₃ plants. *Plant Biology* **6**, 269–279 (2004).

39. Li, Y. S. *et al.* Study on response to potassium (K) application and recommendation of optimal K rates for rapeseed in Hubei. *Chin. J. Oil Crop Sci.* **30**, 469–475 (2008).
40. Lancashire, P. D. *et al.* A uniform decimal code for growth stages of crops and weeds. *Ann. Appl. Biol.* **119**, 561–601 (1991).
41. Genty, B., Briantais, J. M. & Baker, N. R. The relationship between the quantum yield of photosynthetic electron transport and quenching of chlorophyll fluorescence. *BBA-Gen. Subjects* **990**, 87–92 (1989).
42. Li, Y., Gao, Y. X., Xu, X. M., Shen, Q. R. & Guo, S. W. Light-saturated photosynthetic rate in high-nitrogen rice (*Oryza sativa* L.) leaves is related to chloroplastic CO₂ concentration. *J. Exp. Bot.* **60**, 2351–2360 (2009).
43. Manter, D. K. & Kerrigan, J. A/C_i curve analysis across a range of woody plant species: influence of regression analysis parameters and mesophyll conductance. *J. Exp. Bot.* **55**, 2581–2588 (2004).
44. Albertsson, P.-A. A quantitative model of the domain structure of the photosynthetic membrane. *Trends Plant Sci.* **6**, 349–354 (2001).
45. Warren, C. R. The photosynthetic limitation posed by internal conductance to CO₂ movement is increased by nutrient supply. *J. Exp. Bot.* **55**, 2313–2321 (2004).
46. Harley, P. C., Loreto, F., Di Marco, G. & Sharkey, T. D. Theoretical considerations when estimating the mesophyll conductance to CO₂ flux by analysis of the response of photosynthesis to CO₂. *Plant Physiol.* **98**, 1429–1436 (1992).
47. Brooks, A. & Farquhar, G. D. Effect of temperature on the CO₂/O₂ specificity of ribulose-1, 5-bisphosphate carboxylase/oxygenase and the rate of respiration in the light. *Planta* **165**, 397–406 (1985).
48. von Caemmerer, S., Evans, J., Hudson, G. & Andrews, T. J. The kinetics of ribulose-1,5-bisphosphate carboxylase/oxygenase *in vivo* inferred from measurements of photosynthesis in leaves of transgenic tobacco. *Planta* **195**, 88–97 (1994).
49. Farquhar, G. D., von Caemmerer, S. V. & Berry, J. A. A biochemical model of photosynthetic CO₂ assimilation in leaves of C₃ species. *Planta* **149**, 78–90 (1980).
50. Sharkey, T. D., Bernacchi, C. J., Farquhar, G. D. & Singsaas, E. L. Fitting photosynthetic carbon dioxide response curves for C₃ leaves. *Plant Cell Environ.* **30**, 1035–1040 (2007).
51. Gu, L. H. & Sun, Y. Artefactual responses of mesophyll conductance to CO₂ and irradiance estimated with the variable *J* and online isotope discrimination methods. *Plant Cell Environ.* **37**, 1231–1249 (2014).
52. Thomas, R. L., Sheard, R. W. & Moyer, J. R. Comparison of conventional and automated procedures for nitrogen, phosphorus, and potassium analysis of plant material using a single digestion. *Agron. J.* **59**, 240–243 (1967).
53. Huang, Z. A., Jiang, D. A., Yang, Y., Sun, J. W. & Jin, S. H. Effects of nitrogen deficiency on gas exchange, chlorophyll fluorescence, and antioxidant enzymes in leaves of rice plants. *Photosynthetica* **42**, 357–364 (2004).
54. Elstner, E. F. & Heupel, A. Inhibition of nitrite formation from hydroxylammoniumchloride: a simple assay for superoxide dismutase. *Anal. Biochem.* **70**, 616–620 (1976).
55. Chance, B. & Maehly, A. Assay of catalases and peroxidases. *Methods enzymol.* **2**, 764–775 (1955).
56. Meng, F. J., Peng, M., Pang, H. y. & Huang, F. L. Comparison of photosynthesis and leaf ultrastructure on two black locust (*Robinia pseudoacacia* L.). *Biochem. Syst. Ecol.* **55**, 170–175 (2014).
57. Craven, D., Gulamhussein, S. & Berlyn, G. Physiological and anatomical responses of *Acacia koa* (Gray) seedlings to varying light and drought conditions. *Environ. Exp. Bot.* **69**, 205–213 (2010).
58. Makino, A., Mae, T. & Chira, K. Colorimetric measurement of protein stained with coomassie brilliant blue ron sodium dodecyl sulfate–polyacrylamide gel electrophoresis by eluting with formamide. *Agric. Biol. Chem.* **50**, 1911–1912 (1986).
59. Chen, T. W., Kahlen, K. & Stützel, H. Disentangling the contributions of osmotic and ionic effects of salinity on stomatal, mesophyll, biochemical and light limitations to photosynthesis. *Plant cell environ.* doi: 10.1111/pce.12504 (2015).

Acknowledgements

This work was supported by the earmarked fund for China Agriculture Research System (CARS-13); the Special Fund for Agro-scientific Research in the Public Interest (201203013); and the PhD Candidate Research Innovation Project of Huazhong Agricultural University (2014bs17).

Author Contributions

Z.L., T.R. and J.L. conceived and designed the experiment. Z.L. and Y.P. performed the experiments, Z.L. analyzed the data, wrote the main manuscript text and prepared all of the figures, and Z.L., T.R., Y.P., X.L., R.C. and J.L. reviewed and approved the manuscript.

Additional Information

Supplementary information accompanies this paper at <http://www.nature.com/srep>

Competing financial interests: The authors declare no competing financial interests.

How to cite this article: Lu, Z. *et al.* Differences on photosynthetic limitations between leaf margins and leaf centers under potassium deficiency for *Brassica napus* L. *Sci. Rep.* **6**, 21725; doi: 10.1038/srep21725 (2016).



This work is licensed under a Creative Commons Attribution 4.0 International License. The images or other third party material in this article are included in the article's Creative Commons license, unless indicated otherwise in the credit line; if the material is not included under the Creative Commons license, users will need to obtain permission from the license holder to reproduce the material. To view a copy of this license, visit <http://creativecommons.org/licenses/by/4.0/>